Mapping of Low- and High-Fluence Autophosphorylation Sites in Phototropin 1†

Michael Salomon, Elke Knieb, Tibor von Zeppelin, and Wolfhart Rüdiger*

Department of Biology I, Botany, Menzingerstrasse 67, D-80638 München, Germany

Received December 9, 2002; Revised Manuscript Received February 13, 2003

ABSTRACT: Phototropins, originally detected by their blue light-dependent autophosphorylation, are plant photoreceptors involved in several blue light responses such as phototropism, chloroplast relocation, leaf expansion, rapid inhibition of hypocotyl growth, and stomatal opening. Three domains have been identified in phototropin sequences, two chromophore binding domains (LOV1 and LOV2) and a kinase domain. We describe here two additional domains, the N-terminus upstream of LOV1 and the hinge region between LOV1 and LOV2, as the regions for autophosphorylation; the phosphorylation sites were identified by site-directed mutagenesis as S27, S30, S274, S300, S317, S325, S332, and S349 of the PHOT1a sequence of *Avena sativa*. Investigation of the autophosphorylation in vivo revealed that serines close to the LOV1 domain are phosphorylated at lower fluence of blue light than the serines close to the LOV2 domain. Recovery of phosphorylation in vivo during a dark period after saturating irradiation is caused by dephosphorylation rather than by degradation of the phosphorylated form and new synthesis of nonphosphorylated phototropin. The results were obtained by a combination of autophosphorylation of phototropin with phosphorylation of recombinant domains by protein kinase A, which turned out to have the same site specificity as the phototropin kinase, followed by proteolysis and separation of phosphopeptides. With the knowledge of the phosphorylation sites, the physiological and biochemical consequences of autophosphorylation can now be approached by site-directed mutagenesis of phototropins.

Phototropins are a family of UV-A/blue light receptors that are characterized by their common domain structure of two FMN-binding and light-sensing PAS domains, designated as LOV1 and LOV2, in the amino-terminal half and a signal-transmitting serine/threonine kinase in the carboxy-terminal half (*1*, *2*). This kinase becomes activated in response to absorption of UV-A/blue light by FMN in the LOV domains, resulting in autophosphorylation of multiple serine residues.

Early studies in the field of phototropin research were almost exclusively concerned with the characterization of this light-induced phosphorylation response (*3*), and over the years a body of correlative evidence for an essential role of this response in the signaling pathway for phototropism was collected (for a review, see ref *4*). An essential argument for such a correlation was the detection of asymmetric phosphorylation of a membrane protein in oat coleoptiles upon unilateral irradiation (*5*, *6*). The identification of this protein as the photoreceptor for phototropism was achieved when the *PHOT1* gene (at first named *NPH1 for n*on*p*hototropic *h*ypocotyl) was isolated from *Arabidopsis thaliana* (*7*). While radiolabeling in early investigations with crude plant extracts could have been caused by phosphorylation of phototropin by other protein kinases in the extract after activation by blue light, the finding of a signature of a kinase domain in the *PHOT1* gene (*7*) and blue light-induced radiolabeling of phototropin after expression of its cDNA in insect cells indicated autophosphorylation of phototropin (*8*). In the meantime, *PHOT1* genes and related *PHOT2* genes that were previously named *NPL1* for *NPH1 l*ike (*9*) have been described for many plants, and mutant studies showed that the *PHOT* genes encode photoreceptors that are involved not only in phototropism but also in the rapid phase of hypocotyl growth inhibition (*10*), leaf expansion (*11*), chloroplast migration, and stomatal opening (*2*, *12*).

The demonstration that the two LOV domains are the chromophore binding domains and bind FMN also when expressed in *Escherichia coli* (*13*) opened up a new area of research. The recombinant LOV2 domain was shown to undergo a unique photocycle that involves the light-mediated, reversible formation of a covalent bond between a cysteine residue and C4a of the flavin isoalloxazine (*14*, *15*), and the kinetics of formation and decay of this adduct were shown for LOV1, LOV2, and LOV1/LOV2 of several plants (*16*−*18*). The three-dimensional structure of a recombinant LOV2 domain was determined (*19*, *20*), and vibration spectroscopy revealed conformational changes in the chromophore and protein (*21*, *22*).

Although these findings have contributed greatly to our understanding of the photochemistry of phototropins, our knowledge concerning the autophosphorylation response is still fairly poor. Even though earlier studies already demonstrated that light-induced autophosphorylation of higher plant phototropins likely occurs on multiple serine residues (*23*, *24*), reliable information on the actual number of these sites and their location within the protein is entirely lacking so far. Blue light-induced autophosphorylation in vivo is accompanied by a shift to lower SDS−PAGE mobility of

† This work was supported by the Deutsche Forschungsgemeinschaft (Ru108/31-3-4) and the Fonds der Chemischen Industrie.

* To whom correspondence should be addressed. E-mail: ruediger@botanik.biologie.uni-muenchen.de. Fax: +49 89 17861 185. Phone: +49 89 17861 244.

10.1021/bi027324f CCC: $25.00
Published on Web 03/19/2003

phototropin (*25*), and matching the time course of dark recovery of phototropism and of phosphorylation in vitro (*26*), the phototropin form showing an apparently smaller molecular mass is detected again. However, it was not known whether the reappearance of the more rapidly migrating form and the disappearance of the more slowly migrating form were the consequence of degradation of the latter and de novo synthesis of the former or simply dephosphorylation of the latter. This work is aimed at providing answers to these open questions, in particular with regard to the identification of the autophosphorylation sites in PHOT1 and the dynamics of the forward and reverse reactions.

MATERIALS AND METHODS

Plant Growth, Cell Extract Preparation, and Phosphorylation. Avena sativa L. (cv Tomba) seedlings were grown on vermiculite for 4 days at 25 °C in the dark. The procedure for cell extraction and phosphorylation of the crude extract followed that described by Salomon et al. (*5*, *6*). In brief, the coleoptiles were cut just below the node. If required, samples of four coleoptiles were irradiated at a blue light fluence of 1, 10, and 50 μmol m^{-2}. For this purpose, the samples were placed on the bottom of a silver-plated dewar vessel to guarantee uniform irradiation of the tissue; the irradiation time, fixed at 1, 5, and 10 s with a camera shutter, was followed by a dark period of 90 s to allow for in vivo phosphorylation, and the samples were then immediately frozen in liquid nitrogen. For each in vitro phosphorylation reaction, radiolabeled ATP was added to the thawed sample at the same moment as the saturating irradiation with blue light was turned on. The reaction was stopped after 1 min with SDS sample buffer and heating to 90 °C for 3 min, and aliquots were separated on 8% polyacrylamide gels. The position of the phosphorylated phototropin band and the amount of its radioactivity were determined using a phosphoimager (BAS 1500, Fujifilm, Kanagawa, Japan). The phototropin bands were cut out, and the protein was eluted by mincing the gel slices with 3 volumes of 50 mM HEPES−KOH, pH 8.0, containing 5 mM $MgSO_4$ and 0.1% SDS, and heating to 80 °C for 10 min. The gel fragments were removed by centrifugation at 13000*g* for 15 min in a 0.2 μm nanosep tube. The clear eluate was concentrated to the desired volume using microcentrifugal filters with a molecular cutoff of 10 kDa and used for CNBr degradation and tryptic digestion.

Cloning and Site-Directed Mutagenesis of Phototropin Subdomains. Subdomains of phototropin were generated by PCR amplification of the corresponding regions in the PHOT1a cDNA from *A. sativa* (*14*), and site-directed mutagenesis to generate proteins bearing single serine to alanine mutations was carried out according to the QuikChange protocol from Stratagene. The forward/reverse primer combinations are described in the Supporting Information section.

Phosphorylation of Recombinant Phototropin Subdomains with PKA. For phosphorylation of wild-type (WT) and mutated forms of the recombinant N-terminal and H1 regions from oat phototropin, 10 μg of the affinity-purified proteins was incubated in 20 mM Tris-HCl, 150 mM NaCl, 5 mM $CaCl_2$, 10 mM $MgCl_2$, pH 8.4, 0.1 mM ATP, 2 pmol of [γ-^{32}P]ATP (3000 Ci/mmol), and 40 units of the catalytic subunit of protein kinase A (PKA;[1] no. 2645, Sigma, Taufkirchen, Germany), dissolved in 10 μL of 40 mM dithiothreitol, in a total reaction volume of 40 μL for 2 h at 30 °C. The samples were then supplied with 60 μL of a saturated solution of $(NH_4)_2SO_4$, placed on ice for 30 min, and centrifuged for 30 min at 14000*g*. The precipitated phosphorylated proteins were dissolved in 200 μL of 150 mM Tris-HCl, pH 8.8, and 0.1% SDS and incubated for 10 min at 90 °C. Residual-free ATP was removed by exchanging the buffer two times using microcentrifugal filters with a molecular cutoff of 10 kDa. After the final concentration step sample volumes were adjusted to 300 μL with 150 mM Tris-HCl, pH 8.8, and 0.1% SDS.

CNBr Cleavage. To the protein sample, dissolved in 90 μL of gel elution buffer, were added 210 μL of 100% formic acid and 60 μL of a solution of CNBr (Merck, Darmstadt, Germany) in 70% formic acid (300 mg/mL). The mixture was incubated for 2 h at room temperature. The solvent was removed by evaporation under reduced pressure. Addition of a small volume of water and evaporation were repeated until the last traces of acid were removed.

Tryptic Digests. For tryptic digests of either CNBr-cleaved native oat phototropin or the recombinant phototropin subdomains, we usually used 2 μL of the phosphorylated proteins, which were added to 10 μL of a solution containing 150 mM Tris, pH 8.8, 0.1% SDS, 2.5 mM $CaCl_2$, and 5−10 μg of trypsin. The samples were incubated at 37 °C for a minimum of 16 h.

Two-Dimensional Thin-Layer Electrophoresis and Chromatography. For electrophoretic phosphopeptide separation in the first dimension we used a LKB Multiphore II apparatus. Between 1 and 2 μL of a tryptic digest was spotted near the cathode side onto a 20 × 20 cm cellulose thin-layer plate (Polygram CEL 400, UV_{254}) soaked with electrophoresis buffer (1% ammonium carbonate, pH 8.9). Electrophoresis was carried out for 130 min at 500 V and 10 mA. The plates were dried for 5 min with a hair dryer before being placed in a chromatography tank containing a 7.5:5:1.5:6 mixture of 1-butanol, pyridine, glacial acetic acid, and deionized water as a solvent for peptide separation in the second dimension. Chromatography was finished when the solvent front had reached about 1 cm from the top of the plate. The dried plates were then exposed overnight on a BAS-MP imaging screen (Fujifilm, Tokyo, Japan), and the phosphopeptide patterns were evaluated using a beta-scanner phosphorimager (BAS 1500; Fujifilm, Tokyo, Japan) and the programs BAS-Reader and TINA from Raytest (Isotopenmessgeräte GmbH, Straubenhardt, Germany).

RESULTS

Phosphopeptide Pattern of Autophosphorylated Phototropin (PHOT1) from Oat. As a first step in determining the number of sites that become phosphorylated in response to light, we performed the phosphorylation reaction in cell extracts from etiolated oat coleoptiles in vitro in the presence of [γ-^{32}P]ATP under saturating blue light (≫1000 μmol m^{-2}) to induce phosphorylation at all sites. In the dark control, no radioactive band was detectable at the site of the PHOT1

[1] Abbreviations: CBP, calmodulin binding protein; PKA, protein kinase A; WT, wild type.

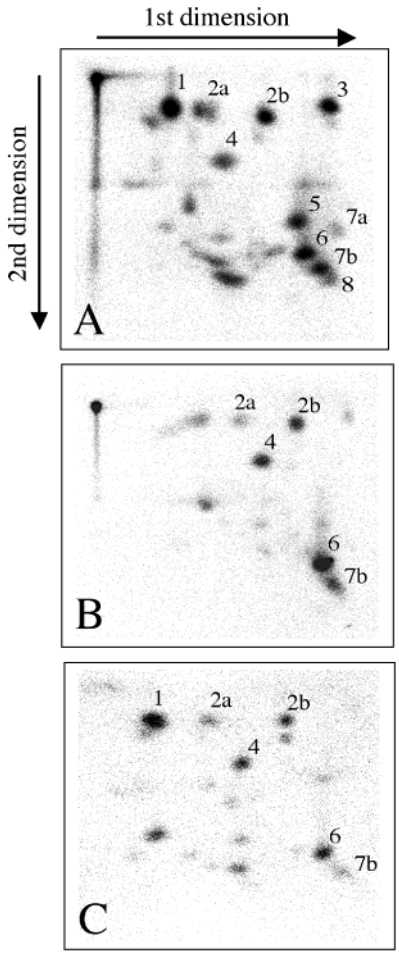

FIGURE 1: Tryptic phosphopeptide pattern of oat phototropin phosphorylated in vitro using cell extracts from the uppermost 5 mm of the coleoptile. (A) The cell extract was subjected to autophosphorylation in the presence of [γ-^{32}P]ATP. The PHOT1 protein was isolated by SDS−PAGE, cleaved with CNBr, and digested with trypsin. The resulting phosphopeptides were separated in the first dimension by electrophoresis in 1% ammonium carbonate buffer at pH 8.9 and in the second dimension by ascending solvent chromatography in 1-butanol/pyridine/acetic acid/water (7.5:5:1.5:6 v/v/v/v). Phosphopeptide spots typically detectable under those conditions are numbered from 1 through 8. (B) Autophosphorylation in vitro was carried out as described in (A), but prior to extraction the coleoptile tips were irradiated with 50 μmol m^{-2} of blue light to induce partial phototropin phosphorylation in vivo. (C) The coleoptile tips were subjected to saturating irradiation and a 20 min dark period before extraction. Autophosphorylation was carried out as in (A).

band that was localized by immunoblotting (data not shown); thus our investigation dealt only with blue light-induced phosphorylation that had been characterized as phototropin autophosphorylation (*8*). After separation on SDS gels, excision of the phosphorylated PHOT1 band, and elution of the protein from the gel slices, we digested the phosphoprotein and analyzed the resulting phosphopeptides by two-dimensional thin-layer electrophoresis and chromatography (2-D TLC). In our initial experiments with trypsin, we found that the majority of the radioactive label did not move from the origin of sample application, indicating that the tryptic digest was incomplete even after repeated incubation with trypsin. However, the treatment of phosphorylated PHOT1 with CNBr significantly improved the results of the subsequent trypsin digestion, and we finally obtained a reproducible and reliable phosphopeptide pattern (Figure 1A). In total there were 10 labeled spots that were detectable under these conditions in all of our experiments. The relative labeling was highest at spot 1 and decreased in the following order: spots 2a + 2b, 6, 3, 7a + 7b, 5, 4, and 8 (see Figure 2A, dark control). The unequal distribution of the radioactivity, in particular with regard to the weakly labeled spots, can be explained either by incomplete phosphorylation at some sites or by inefficient cleavage resulting in multiple digestion products. It will be shown below that peptides 2a and 2b are derived from the same phosphorylation site, and the same applies to peptides 7a and 7b. Thus, the 10 labeled spots indicate a total of 8 phosphorylation sites.

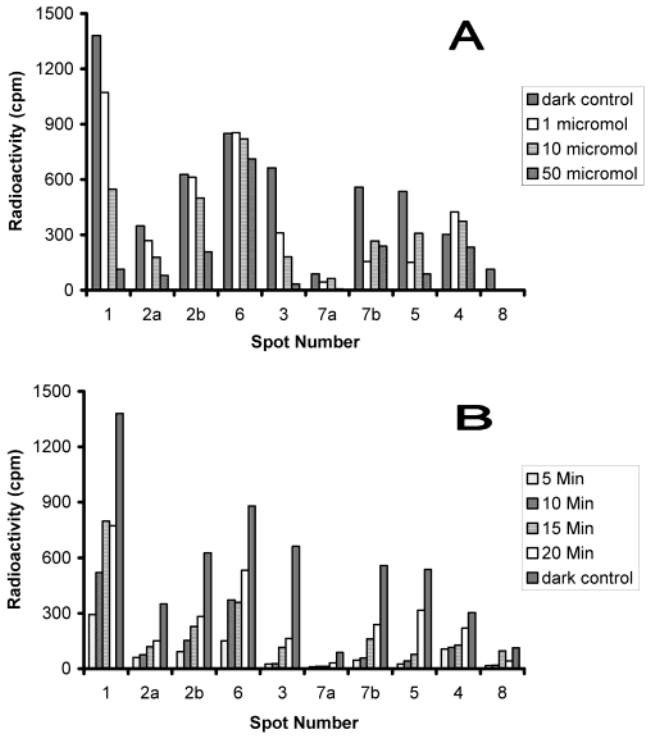

FIGURE 2: Evaluation of the occupation of single phosphorylation sites in vivo by in vitro phosphorylation of PHOT1 with [γ-^{32}P]-ATP. For spot numbers see Figure 1. (A) The phosphorylation in vitro was carried out immediately after illumination of coleoptiles with 1, 10, and 50 μmol m^{-2} of blue light. The decrease of label indicates in vivo phosphorylation with endogenous, nonradioactive ATP. (B) The coleoptiles were subjected to saturating illumination to induce maximum phosphorylation with endogenous, nonradioactive ATP, followed by dark periods of 5, 10, 15, and 20 min and subsequent in vitro phosphorylation with [γ-^{32}P]ATP. The radioactivity indicates in vivo recovery of phosphorylation.

Fluence-Dependent Autophosphorylation and Time-Dependent Dephosphorylation of Phototropin. To test whether all phosphorylation sites respond to light activation in the same manner, we irradiated oat coleoptiles in vivo with increasing fluences of blue light reaching from 1 to 50 μmol m^{-2} to induce partial phototropin autophosphorylation with endogenous nonradioactive ATP. Subsequently, we subjected the cell extracts prepared from these tissues to radioactive phosphorylation in vitro followed by 2-D TLC analysis of the phosphopeptides obtained by CNBr cleavage and trypsin digestion of the isolated PHOT1 protein. If all phosphorylation sites become phosphorylated simultaneously, independent of the fluence, the radioactive label of all spots should decrease equally with increasing in vivo fluence. On

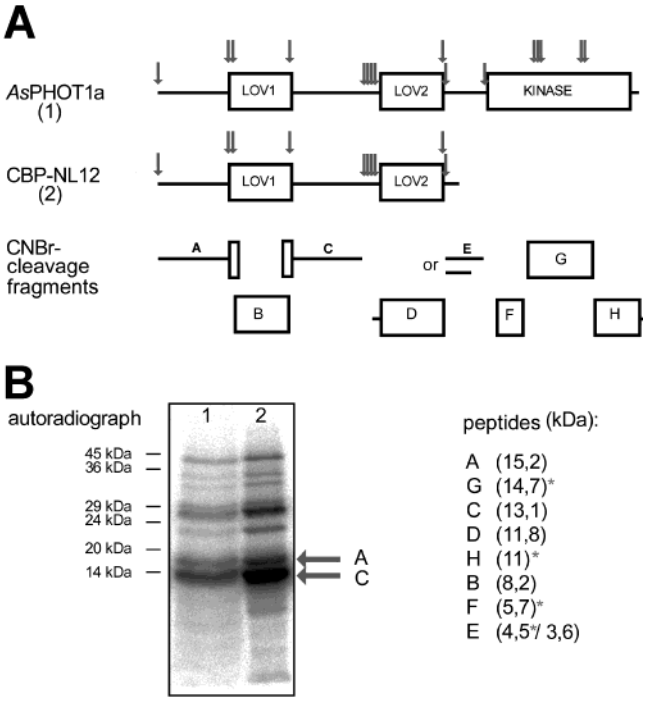

FIGURE 3: Cyanobromide degradation of PHOT1 from oat (1) and the recombinant fragment CBP-NL12 (2). (A) The arrows indicate the position of Met residues in both sequences, and CNBr cleavage results in fragments A−H. (B) SDS−PAGE of CNBr cleavage fragments obtained from PHOT1 after autophosphorylation (lane 1) and from CBP-NL12 after phosphorylation with PKA (lane 2). Only peptides of the size of fragments A (containing the N-terminus) and C (containing the H1 region) are phosphorylated; we assume that larger fragments result from incomplete CNBr degradation. For comparison, all expected CNBr cleavage fragments are listed in order of their size. An asterisk designates peptide fragments not present in the digest of CBP-NL12.

the other hand, if there is a higher sensitivity of some sites for low fluences, these should disappear in the 2-D TLC first while in vitro labeling of others should still be possible. We found indeed that labeling of some spots disappeared while others were still detectable (Figure 1B). A more detailed analysis showed that labeling of spots 3, 5, 7a + 7b, and 8 disappeared earlier than that of spots 1 and 2a + 2b while spots 4 and 6 did not lose much label through irradiation up to a fluence of 50 μmol m^{-2} (Figure 2A). For investigation of recovery of phosphorylation in vivo, the oat coleoptiles were subjected to saturating irradiation to induce complete phosphorylation with nonradioactive ATP and incubated in darkness for 5−20 min before the cell extract was prepared for immediate radioactive phosphorylation in vitro. The 2-D TLC analysis (Figure 1C) showed that some spots reappeared before the others, and a detailed analysis indicated reappearance in the order of spots 1, 2a + 2b, 4, and 6 before the others (Figure 2B). Spot 8 did not show up even within 20 min of dark incubation. Thus, the order of recovery in a dark period after irradiation seems to be the opposite of the order of the fluence-dependent phosphorylation for most phosphorylation sites.

The Same Phototropin Domains Are Targets for Autophosphorylation and for Protein Kinase A (PKA). To find out which domains contain phosphorylation sites, we subjected phototropin after autophosphorylation and CNBr cleavage to SDS−PAGE. According to the position of Met residues within the sequence shown in Figure 3A, CNBr fragments A−E are expected, corresponding to the N-terminal domain, the LOV1 domain, the hinge 1 region, the LOV2 domain, and the hinge 2 region, respectively, while the kinase domain should be cleaved into fragments F−H. The autoradiograph (Figure 3B, lane 1) shows a relatively simple pattern of labeled bands; the highest label was found at 13 kDa, the size of fragment C comprising the H1 region, followed by the label at about 16 kDa, close to the size of fragment A containing the N-terminal domain. The labeled bands which are larger than the expected fragments, e.g., the 29 kDa band, must result from incomplete CNBr cleavage; it can be speculated that they result from a combination of fragments A and C with neighboring fragments although other explanations are still possible at this point. Radioactivity was not detectable at the position of smaller fragments corresponding to LOV1, LOV2, hinge 2, and two kinase fragments (for the size see Figure 3B). Labeling of kinase fragment G (14.7 kDa) should result in a labeled band between those of fragments A and C. No such extra band was observed, indicating either that the resolution of the gel system was insufficient to separate fragment G from fragment A or that one of these bands was not phosphorylated.

Autophosphorylation is not a suitable approach for determination of phosphorylation sites by point mutation because lacking phosphate incorporation in a mutant can be caused not only by removal of the phosphorylation site but also by impaired kinase activity in this case. Heterologous phosphorylation with a kinase showing the same specificity as phototropin is required for such an approach. Since the recombinant kinase domain of phototropin turned out to be inactive in our hands, we used PKA instead, which is homologous to the phototropin kinase domain (>40% sequence identity); hence, there is a certain probability that it recognizes the same phosphorylation sites as phototropin. To avoid any unwanted autophosphorylation, we used the clone CBP-NL12, a phototropin without the kinase domain (see Figure 3A), as substrate. The control experiment without PKA did not show any detectable protein phosphorylation (data not shown). The pattern of CNBr fragments (Figure 3B, lane 2) proved to be identical with that of the fragments from autophosphorylated phototropin (Figure 3B, lane 1). This means that only fragments A and C contain the phosphorylation sites of CBP-NL12; the identical size renders fragments A and C the best candidates for the corresponding bands also in lane 1 although the participation of fragment G cannot be excluded at this point.

To test this conclusion further, we cloned cDNA fragments containing the single phototropin domains [the N-terminal domain (aa 1−132), the LOV1 domain (aa 133−243), the hinge 1 region (H1) (aa 244−412), the LOV2 domain (aa 413−520), the hinge 2 region (H2) (aa 521−593), and the C-terminal kinase (aa 594−923)] (see Figure 4A) of the PHOT1a cDNA from *A. sativa* into the *E. coli* expression vector pCALn and tested the resulting fusion proteins containing the calmodulin binding protein (CBP) in the phosphorylation assay with PKA. Here also, no protein phosphorylation was detectable without PKA. Since CBP contains phosphorylation sites, the true label of the single domains became apparent only after digestion with thrombin (Figure 4B). We confirmed that the N-terminal and H1 domains were phosphorylated; the weak radioactivity of

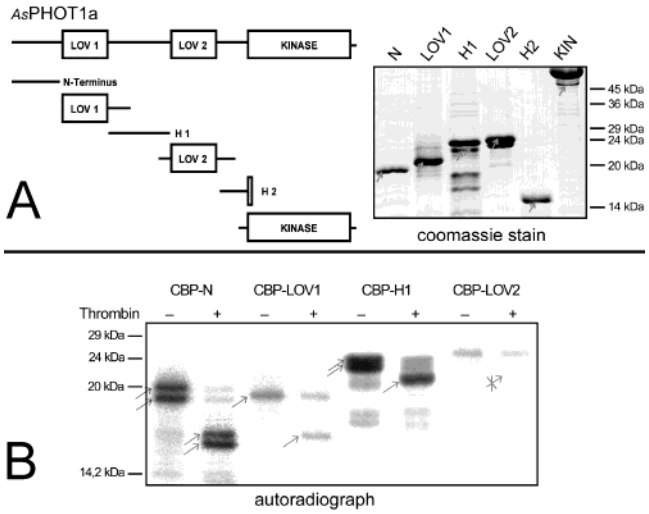

FIGURE 4: Investigation of single recombinant domains of PHOT1a from oat. (A) Scheme (left) and SDS−PAGE (right) of the recombinant domains indicating successful expression of all domains. (B) In vitro phosphorylation of the single domains with PKA and [γ-^{32}P]ATP. After removal of the calmodulin binding protein (CBP) with thrombin, only the N-terminus and the H1 region retain strong label. The recombinant peptide labeled LOV1 contains part of the H1 domain including S274, which is a phosphorylation site (see Figure 6).

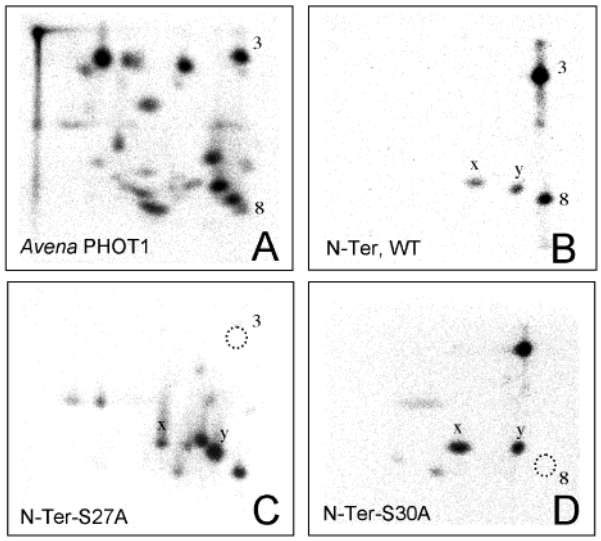

FIGURE 5: Assignment of phosphorylation sites in the N-terminal domain of PHOT1. (A) Phosphopeptide pattern obtained by autophosphorylation of PHOT1 (see Figure 1A). (B−D) Pattern obtained by phosphorylation of the fusion protein CBP-N with PKA. (B) WT = wild type; phosphopeptides 3 and 8 are derived from the N-terminus and phosphopeptides x and y from CBP. (C) Phosphopeptide 3 disappeared in the mutant S27A. (D) Phosphopeptide 8 disappeared in the mutant S30A.

LOV1 can be explained by the presence of 32 amino acids, including S274, belonging to H1 in the investigated LOV1 clone. No label was detectable in LOV2 (Figure 4B), hinge 2, and the kinase domain (data not shown). The latter result supports the assumption that CNBr fragments A and C were labeled as shown in Figure 3B and that fragment G that is part of the kinase domain was not phosphorylated.

Phosphopeptide Pattern of the PHOT1 N-Terminal and H1 Subdomains Phosphorylated by PKA. The subsequent 2-D TLC analysis of the PKA-phosphorylated N-terminal and H1 region yielded phosphopeptides with mobilities, both in the first and in the second dimension, identical to those found for the native protein. For the N-terminus we obtained four different spots. The mobility of one spot equals that of spot 3 while a second spot exhibits the properties of spot 8 of oat PHOT1 (Figure 5A,B). Phosphopeptides x and y were found in all CBP-containing fusion proteins and likely result from CBP phosphorylation. The 2-D coordinates of phosphopeptides obtained from H1 are, except for x and y, in excellent agreement with those of phosphopeptides 1, 2a, 2b, 4, 5, 6, 7a, and 7b of PHOT1 (Figure 6A,B). Thus, PKA apparently phosphorylates the same sites as the phototropin kinase, indicating that both enzymes have similar or even identical substrate specificities; further, the result confirms that all phosphorylation sites of phototropin autophosphorylation are present in the N-terminus and H1.

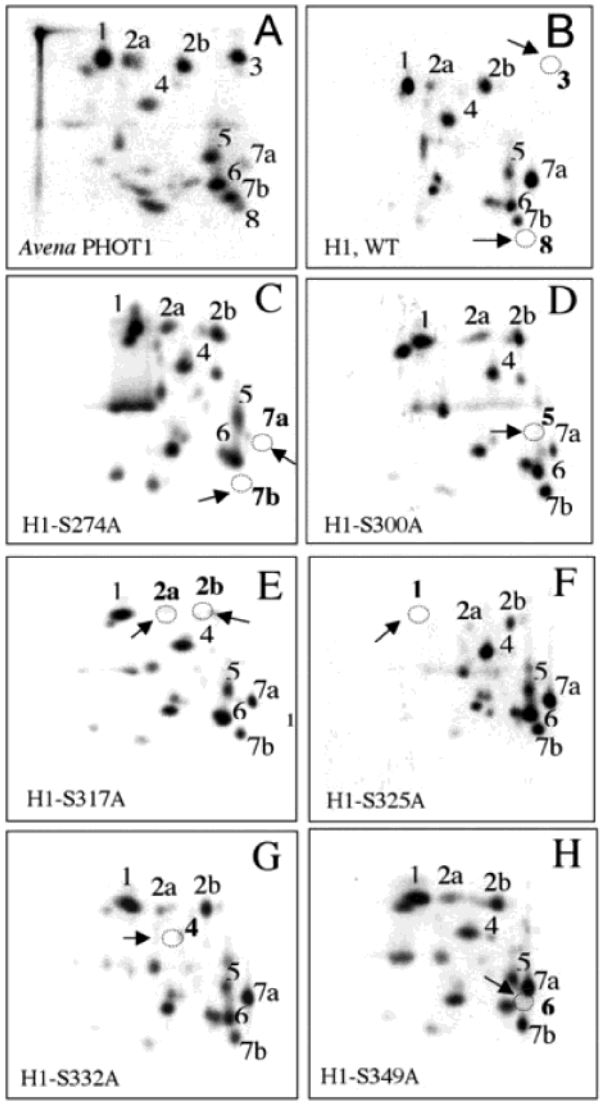

FIGURE 6: Assignment of phosphorylation sites in the H1 region of PHOT1. (A) Phosphopeptide pattern obtained by autophosphorylation of PHOT1 (see Figure 1A). (B−H) Pattern obtained by phosphorylation of the fusion protein CBP-H1 with PKA; spots x and y, derived from CBP, are not marked. Arrows indicate the spots that disappear by mutation. (B) WT showing signals for spots 1, 2a, 2b, 4, 5, 6, 7a, and 7b. (C) Spots 7a and 7b disappeared in mutant S274A. (D) Spot 5 disappeared in mutant S300A. (E) Spots 2a and 2b disappeared in mutant S317A. (F) Spot 1 disappeared in mutant S325A. (G) Spot 4 disappeared in mutant S332A. (H) Spot 6 disappeared in mutant S349A.

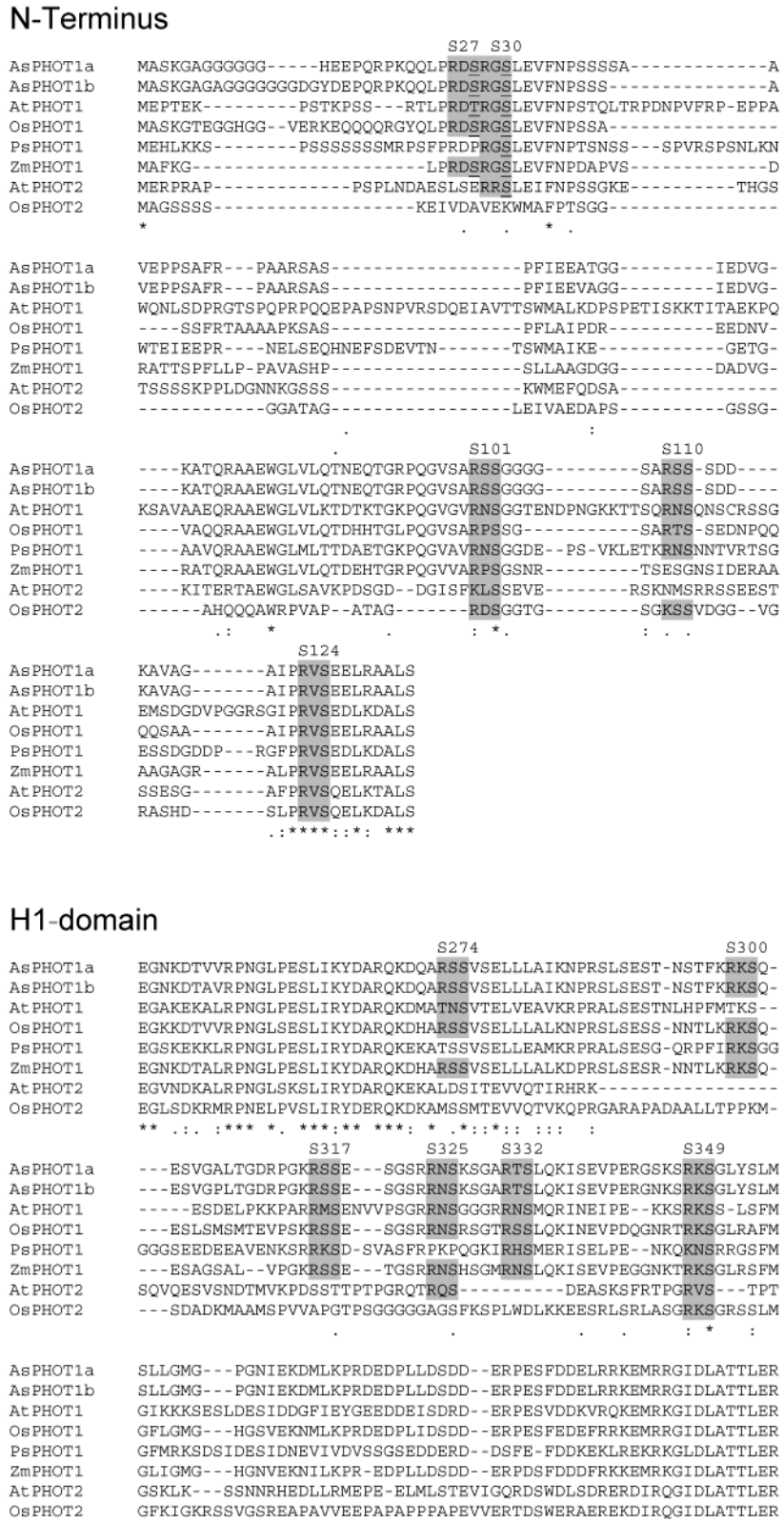

FIGURE 7: Alignment of the N-terminal and H1 domains of higher plant PHOT1 proteins from *A. sativa* (*As*PHOT1a and *As*PHOT1b), *A. thaliana* (*At*PHOT1), *Oryza sativa* (*Os*PHOT1), and *Pisum sativum* (*Ps*PHOT1) and the two PHOT2 homologues from *A. thaliana* (*At*PHOT2) and *O. sativa* (*Os*PHOT2). Conserved putative phosphorylation motifs are shaded in gray. Positions of serine residues in *As*PHOT1a that could function as sites for phototropin autophosphorylation are indicated above the gray-shaded boxes.

Identification of Phosphorylation Sites within the PHOT1 N-Terminus and H1 Domain. A recognition motif frequently phosphorylated by PKA is RxS (*27*). A sequence analysis of the two phototropin domains that we found to be PKA substrates showed five conserved RxS motifs in the N-terminal region, serines 27, 30, 101, 110, and 124, and six conserved RxS motifs in the H1 region, serines 274, 300, 317, 325, 332, and 349 (Figure 7).

To assign the phosphopeptides determined for the N-terminus to particular phosphorylation sites, we then ex-

changed serines 27, 30, 101, 110, and 124 for alanine by site-directed mutagenesis. The PKA reaction with equal amounts of each fusion protein yielded reduced phosphate incorporation in mutants S27A (66% of WT) and S30A (51% of WT) while mutants S101A, S106A/S110A, and S124A retained the degree of WT phosphorylation. Thus S27 and S30 are likely the only phosphorylation sites in the N-terminal domain. In accordance with this result, the phosphopeptide pattern, obtained by digestion of mutated proteins S101A, S106A/S110A, and S124A, was identical with that of WT (data not shown) while replacement of serine 27 with alanine resulted in the disappearance of spot 3 and replacement of serine 30 with alanine resulted in the disappearance of spot 8 (Figure 5C,D). For the S27A mutant protein an additional spot appears just below and to the right of spot y that is not present in the WT protein. The most likely explanation is that this phosphopeptide represents a partial tryptic digestion product containing residue 30.

We then replaced each conserved serine within the putative phosphorylation motifs depicted in Figure 7 respectively with alanine for the recombinant H1 region as well. Since the phosphate incorporation into the single mutated fusion proteins was only marginally reduced, we concentrated our efforts upon phosphopeptide analysis. Elimination of serine 274 resulted in the disappearance of spots 7a and 7b, and phosphopeptides 5, 2a + 2b, 1, 4, and 6 disappeared in the mutant proteins S300A, S317A, S325A, S332A, and S349A, respectively (Figure 6C−H). A comparison of these results with the phosphopeptide map determined for the native photoreceptor allows the unequivocal assignment of spot 1 to S325, spots 2a and 2b to S317, spot 4 to S332, spot 5 to S300, spot 6 to S349, and probably spots 7a and 7b to S274 although the separation of spots 7a and 7b from spots 5 and 8 proved to be difficult.

The Mobility Shift and Loss of Immunoreaction of Oat Phototropin Are the Result of Phosphorylation at the N-Terminus. Several interesting observations confirm that serines 27 and 30 are phosphorylated in the native protein. An antiserum raised against the N-terminal part of *A. thaliana* PHOT1 showed strong cross-reactivity with PHOT1 from dark-grown *A. sativa* seedlings but not with phosphorylated PHOT1, i.e., from etiolated oat seedlings that were irradiated with saturating blue light prior to harvest (Figure 8A). The same is true for maize PHOT1 but not for the photoreceptor from dicot plants: the antiserum recognizes also the phosphorylated form of PHOT1 from *Arabidopsis*, mustard, pea, and cress (data not shown). The antiserum reacted also with the recombinant N-terminal domain of oat PHOT1 but did not do so after phosphorylation by PKA (Figure 8B). No reaction was observed with a double mutant that lacked both serines 27 and 30 (Figure 8B). This finding can be reasonably explained on assuming that the cross-reaction to monocot PHOT1 of this antiserum requires an epitope around serines 27 and 30. In single mutants, antibody binding was much more affected when serine 30 was eliminated than in the absence of serine 27 (Figure 8C). Further, Figure 8B shows a reduced electrophoretic mobility of the N-terminus of oat phototropin on phosphorylation with PKA. Such a shift was not found for the S30A mutant protein but was detectable for the S27A mutation, although to a somewhat reduced degree. It has been reported by several authors that autophosphorylated phototropin exhibits a reduced electrophoretic mobility; we show here that this effect is most likely caused by phosphorylation at S30 and, to a lesser extent, at S27. Together, the above-described TLC, antibody, and in vitro phosphorylation studies of the oat PHOT1 N-terminal domain provide clear evidence that S27 and S30 are the only target sites in the N-terminus for PKA and probably also for the PHOT1 kinase; they correspond to spots 3 and 8, respectively, of the 2-D TLC analysis.

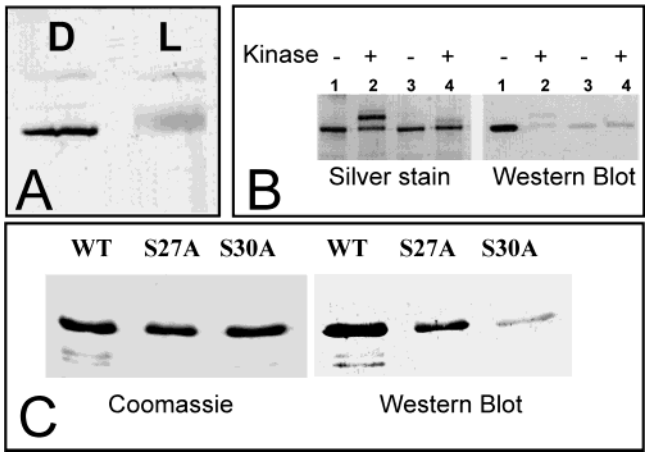

FIGURE 8: Phosphorylation at S30 modifies the electrophoretic mobility and the reaction with antiserum of oat PHOT1. (A) Western blot with oat PHOT1: D = dark, PHOT1 is not phosphorylated; L = light, the signal of PHOT1 almost disappeared. (B and C) Investigation of the fusion protein CBP-N. (B) The mobility shift by phosphorylation is seen in the wild type (lanes 1 and 2, silver stain) but not in the double mutant S27/30A (lanes 3 and 4); the Western blot shows that the reaction with the antiserum nearly disappeared by phosphorylation of the wild type (lanes 1 and 2) and by mutation (lanes 3 and 4). (C) The mutant S27A shows a reduced signal and the mutant S30A almost no detectable signal in the Western blot.

DISCUSSION

Number of Phosphorylation Sites. We have mapped 8 PKA-dependent phosphorylation sites by site-directed mutagenesis in the recombinant N-terminus and H1 region of PHOT1a from oat, and since the pattern of phosphopeptides derived from these 8 sites was also observed in the 2-D TLC analysis of autophosphorylated phototropin, we conclude that these sites are genuine phosphorylation sites of this photoreceptor. We cannot rigorously exclude the presence of additional phosphorylation sites, especially because we occasionally observed other labeled spots in the 2-D TLC analysis of H1 and PHOT. However, a closer look shows that this possibility is not very likely. (1) These additional spots were not always observed, but if they were, some of the identified spots were drastically reduced in their amount. (2) All additional spots were found to migrate only a short distance in the first dimension, indicating relatively high isoelectric points. This is characteristic for phosphopeptides that contain more than one of the basic amino acids (K and/or R). On complete digestion, K or R occurs only once at the C-terminus of each tryptic peptide; the presence of two or more K or R residues in a peptide results from incomplete digestion. (3) The position of phosphopeptides in the 2-D TLC can be predicted using isoelectric points calculated with a program available at http://acrux.igh.cnrs.fr/gs/phospepsort4.html and the aliphatic index using the program http://www.expasy.ch/tools/protparam.html; the pre-

diction matches the observed position of all identified phosphopeptides, assuming partial tryptic cleavage only for peptides 1, 2a, and 7b. The calculation with serines outside the identified sites gave the same result as with the identified serines: the position of the additional spots matches only products of partial tryptic digest. Taken together, these arguments allow the conclusion that the additional spots are caused by products of incomplete tryptic digestion, which can be composed of some of the identified phosphopeptides although the contribution of additional, nonidentified phosphopeptides cannot be excluded. At least for the phosphorylation of recombinant domains with PKA, any contribution of additional sites must be marginal: the double N-terminal mutant S27/30A showed almost no phosphorylation (<1% of WT) and the quadruple H1 mutant S274/300/325/349A, which contains still the phosphorylation sites S317 and S332, showed only less than 2% phosphate incorporation compared to WT (*28*). The finding of traces of phosphothreonine besides phosphoserine by hydrolysis of phosphorylated phototropin (*23*, *24*) may also indicate additional phosphorylation sites in phototropin; if these are threonine residues of phototropin, their contribution to the overall phosphorylation must be marginal; however, the presence of traces of other proteins in the phototropin fraction used for hydrolysis cannot entirely be ruled out.

Low- and High-Fluence Sites of Phosphorylation. Though most of the early biochemical studies of blue light-induced phototropin autophosphorylation revealed a strong correlation with phototropism, one finding was in apparent contrast: the photosensitivity of the phosphorylation response is 1−2 orders of magnitude higher than that for phototropic curvature (*5*, *23*). For a possible explanation, Briggs (*29*) postulated that phototropin phosphorylation may occur in a fluence-dependent manner in that some sites become already phosphorylated in response to very low blue light fluences to trigger phototropic signaling while phosphorylation of the remaining sites requires higher light fluences; the latter event could then be involved in the desensitization of the photoreceptor system. We show here that phototropin contains indeed low- and high-fluence sites for phosphorylation in vivo. Sites S27, S30, S274, and S300 were identified as low-fluence sites and S332 and S349 as high fluence sites; S317 and S325 show intermediate properties. The low-fluence sites are located close to the LOV1 domain, a domain that may play a role in dimerization (M. Salomon and G. Richter, unpublished results) and possibly also as one of the domains for heterologous protein−protein interaction, e.g., with NPH3 (*30*). It is reasonable to assume that the introduction of negative charges by phosphorylation has a strong influence on such interactions. Most phosphorylation motifs are conserved in PHOT1 of different plants (see Figure 7). The high-fluence phosphorylation site around S349 is conserved even in PHOT2. This is perhaps unexpected since PHOT1 and PHOT2 act redundantly as blue light receptors in various responses (*31*, *32*) but appear to exhibit distinct photosensitivities with PHOT2 apparently functioning as a high-fluence receptor (*31*, *33*).

It must be mentioned that low- and high-fluence sites were found for in vivo phosphorylation; preliminary results of in vitro phosphorylation did not show such a preference for low and high fluences of the various phosphorylation sites. Thus, the fluence dependency discussed above is not an intrinsic property of phototropin; environmental factors present in vivo, e.g., attachment to the plasma membrane (*11*) or binding of proteins such as NPH3 (*30*), may play an important role.

Recovery of Phototropism after Irradiation Is Connected with Dephosphorylation of Phototropin. Immediately after a supersaturating irradiation with white light, seedlings do not respond to light that normally induces phototropic curvature; such responsiveness is gradually recovered, however, during a dark period following the supersaturating irradiation. The kinetics of this dark recovery of phototropism closely matches the kinetics of dark recovery of phototropin phosphorylation in vitro (*26*), indicating the gradual disappearance of occupied and appearance of nonoccupied phosphorylation sites in phototropin (see ref *34*). Two models have been discussed for this process: either degradation of the phosphorylated form and new synthesis of the nonphosphorylated form of phototropin or dephosphorylation of phototropin. Any phototropin synthesized in the dark period after the supersaturating irradiation should behave like the phototropin of the dark control that is probably nonphosphorylated and shows a defined capacity for blue light-dependent phosphorylation, reflected by a defined phosphopeptide pattern (see Figure 1A); this pattern should be constant throughout the period of dark recovery. The data of Figure 2B show that this is not the case: the phosphopeptide pattern is different from that of the dark control and changes during the period of dark incubation. However, the results are compatible with the assumption of dephosphorylation of preexisting phototropin; thus, we provide here experimental evidence in favor of this model.

Phosphorylation of the N-Terminus. The N-terminus contains five RxS motifs, most of which are conserved in PHOT1 and PHOT2 from various plants (see Figure 7). Nevertheless, only two of these are phosphorylated with PKA in the recombinant N-terminus of PHOT1a from oat, namely, those containing S27 and S30 (see Figure 5). The other potential phosphorylation sites at S101, S110, and S124 must be inaccessible for PKA, most probably by folding of the peptide chain. Two visible effects are connected with the phosphorylation at S27 and S30, a decrease in mobility of the peptide in SDS−PAGE and nearly complete loss of recognition by an antiserum raised against the N-terminus of *Arabidopsis* PHOT1 (see Figure 8B). An important epitope likely includes the free OH group of S30; almost no immunoreaction was observed with the mutant S30A (Figure 8C). The recombinant H1 region shows almost no mobility shift in SDS−PAGE on phosphorylation (*28*). However, reduced mobility in SDS−PAGE caused by phosphorylation was also described for native phototropin (*4*), and we showed here the disappearance of the immunoreaction of the *Arabidopsis* antiserum with oat phototropin, caused by phosphorylation (see Figure 8A). Thus, these properties of native phototropin are likely determined by the properties of the N-terminus. The situation in vivo seems to be more complex than deduced from the results of in vitro phosphorylation of the recombinant N-terminus: with increasing fluence, the mobility shift of phototropin is detectable before the immunoreaction disappears, and during dark recovery, the immunoreaction appears first and is then followed by disappear-

ance of the mobility shift (*28*). It remains to be shown whether modifications other than phosphorylation of phototropin are involved here.

In summary, we identified 8 phosphorylation sites in phototropin 1, showed their different degree of autophosphorylation in cell extracts, and determined, by an indirect method, the fluence-dependent phosphorylation and the time-dependent dephosphorylation of the different sites. With the knowledge of the phosphorylation sites, the way is open for specific mutagenesis studies to elucidate the physiological consequences of autophosphorylation of phototropins.

ACKNOWLEDGMENT

We thank Winslow Briggs for very helpful comments and suggestions during the process of manuscript preparation. Acknowledging his early work on phototropin phosphorylation, we dedicate this paper to Achim Hager on the occasion of his 75th birthday.

SUPPORTING INFORMATION AVAILABLE

Experimental details including primer sequences used for cloning and site-directed mutagenesis of phototropin subdomains. This material is available free of charge via the Internet at http://pubs.acs.org.

REFERENCES

1. Briggs, W. R., Beck, C. F., Cashmore, A. R., Christie, J. M., Hughes, J., Jarillo, J. A., Kagawa, T., Kanegae, H., Liscum, E., Nagatani, A., Okada, K., Salomon, M., Rüdiger, W., Sakai, T., Takano, M., Wada, M., and Watson, J. C. (2001) *Plant Cell 13*, 993−997.
2. Briggs, W. R., and Christie, J. M. (2002) *Trends Plant Sci. 7*, 204−210.
3. Briggs, W. R., Salomon, M., and Christie, J. M. (2001) *Antioxid. Redox Signaling 5*, 775−788.
4. Short, T. W., and Briggs, W. R. (1994) *Annu. Rev. Plant Physiol. Plant Mol. Biol. 45*, 143−171.
5. Salomon, M., Zacherl, M., and Rüdiger, W. (1997) *Plant Physiol. 115*, 485−491.
6. Salomon, M., Zacherl, M., and Rüdiger, W. (1997) *Bot. Acta 110*, 214−216.
7. Huala, E., Oeller, P. W., Liscum, E., Han, I.-S., Larsen, E., and Briggs, W. R. (1997) *Science 278*, 2121−2123.
8. Christie, J. M., Reymond, P., Powell, G. K., Bernasconi, P., Raibekas, A. A., Liscum, E., and Briggs, W. R. (1998) *Science 282*, 1698−1701.
9. Jarillo, J. A., Ahmad, M., and Cashmore, A. R. (1998) *Plant Physiol. 117*, 719.
10. Folta, K. M., and Spalding, E. P. (2001) *Plant J. 26*, 471−478.
11. Sakamoto, K., and Briggs, W. R. (2002) *Plant Cell 14*, 1723−1735.
12. Kagawa, T., and Wada, M. (2002) *Plant Cell Physiol. 43*, 367−371.
13. Christie, J. M., Salomon, M., Nozue, K., Wada, M., and Briggs, W. R. (1999) *Proc. Natl. Acad. Sci. U.S.A. 96*, 8779−8783.
14. Salomon, M., Christie, J. M., Knieb, E., Lempert, U., and Briggs, W. R. (2000) *Biochemistry 39*, 9401−9410.
15. Salomon, M., Eisenreich, W., Dürr, H., Schleicher, E., Knieb, E., Massey, V., Rüdiger, W., Müller, F., Bacher, A., and Richter, G. (2001) *Proc. Natl. Acad. Sci. U.S.A. 98*, 12357−12361.
16. Swartz, T. E., Corchnoy, S. B., Christie, J. M., Lewis, J. W., Szundi, I., Briggs, W. R., and Bogomolni, R. A. (2001) *J. Biol. Chem. 276*, 36493−36500.
17. Kasahara, M., Swartz, T. E., Olney, M. A., Onodera, A., Mochizuki, N., Fukuzawa, H., Asamizu, E., Tabata, S., Kanegae, H., Takano, M., Christie, J. M., Nagatani, A., and Briggs, W. R. (2002) *Plant Physiol. 129*, 762−773.
18. Holzer, W., Penzkofer, A., Fuhrmann, M., and Hegemann, P. (2002) *Photochem. Photobiol. 75*, 479−487.
19. Crosson, S., and Moffat, K. (2001) *Proc. Natl. Acad. Sci. U.S.A. 98*, 2995−3000.
20. Crosson, S., and Moffat, K. (2002) *Plant Cell 14*, 1067−1075.
21. Iwata, T., Tokutomi, S., and Kandori, H. (2002) *J. Am. Chem. Soc. 2002*, 11840−11841.
22. Swartz, T. E., Wenzel, P. J., Corchnoy, S. B., Briggs, W. R., and Bogomolni, R. A. (2002) *Biochemistry 41*, 7183−7189.
23. Palmer, J. M., Short, T. W., Gallagher, S., and Briggs, W. R. (1993) *Plant Physiol. 102*, 1211−1218.
24. Short, T. W., Porst, M., Palmer, J., Fernbach, E., and Briggs, W. R. (1994) *Plant Physiol. 104*, 1317−1324.
25. Short, T. W., Reymond, P., and Briggs, W. R (1993) *Plant Physiol. 101*, 647−655.
26. Palmer, J. M., Short, T. W., and Briggs. W. R. (1993) *Plant Physiol. 102*, 1219−1225.
27. Hanks S. K., and Hunter, T. (1995) *FASEB J. 9*, 576−596.
28. Knieb, E. (2002) Dissertation, University Muenchen.
29. Briggs, W. R. (1996) in *UV/Blue light: perception and responses in plants and microorganisms*, p 49, University Marburg.
30. Motchoulski, A., and Liscum, E. (1999) *Science 286*, 961−964.
31. Sakai, T., Kagawa, T., Kasahara, M., Swartz, T. E., Christie, J. M., Briggs, W. R., Wada, M., and Okada, K. (2001) *Proc. Natl. Acad. Sci. U.S.A. 98*, 6969−6974.
32. Kinoshita, T., Doi, M., Suetsugu, N., Kagawa, T., Wada, M., and Shimazaki, K.-I. (2001) *Nature 414*, 656−660.
33. Kagawa, T., Sakai, T., Suetsugu, N., Oikawa, K., Ishiguro, S., Kato, T., Tabata, S., Okada, K., and Wada, M. (2001) *Science 291*, 2138−2141.
34. Short, T. W., Porst, M., and Briggs, W. R. (1992) *Photochem. Photobiol. 55*, 773−781.

BI027324F